Magazine of Concrete Research, 1993, **45**, No. 165, Dec., 281–291

Experimental investigation of behaviour of anchorage zones

T. J. Ibell* and C. J. Burgoyne†

CAMBRIDGE UNIVERSITY

This Paper is the first of three on the behaviour of anchorage zones for prestressed concrete. Details of an experimental investigation carried out to determine the behaviour of concrete prisms strip-loaded through rigid steel plates are presented. This loading arrangement represents the transfer of force from tendon to concrete at the anchorage of a prestressed concrete structure. The results of several tests have shown that present design methods of anchorage zones are generally very conservative, which leads to an excessive quantity of steel reinforcement in this highly stressed region, that can lead to poor-quality compaction. It has been found, however, that the spreading of such steel over depths greater than those presently used could perhaps relieve this congestion with little loss in strength of the anchorage. Out-of-plane failures during strip-loading tests were also encountered. Proof must therefore be obtained that such third-direction failure cannot occur in practice if planar failure of the anchorage has been assumed during analysis.

Notation

a	half-breadth of test specimens
a_l	half-length of loading plate
a_l/a	concentration ratio
d	diameter of steel reinforcing bars
f_{cu}	concrete cube compressive strength
f_t'	concrete split-cylinder tensile strength
f_y	yield strength of steel reinforcing bars
h	height of concrete prism
k_e	enhancement factor ($= P/P_0$)
p	applied contact pressure under bearing plate
w	width of test specimens
A_s	total area of reinforcing steel crossing a plane
D_r	depth of reinforcement
E_c	Young's modulus for concrete
P	applied ultimate load capacity
P_{cr}	applied load at first visible cracking
P_0	notional load capacity of unreinforced column
T	total elastic tensile force across central axis of loading
β	half-wedge failure angle (to the vertical)
Φ	steel parameter (defined in equation (1))

* SASOL Technology, South Africa.
† University of Cambridge, Engineering Department, Trumpington St., Cambridge, CB2 1PZ, UK.
Paper received 1 June 1993.

Introduction

The problem of a concentrated anchor-load acting on concrete is fundamentally one of a three-dimensional nature. However, the vast majority of the existing analytically-based methods[1–8] have been developed for the two-dimensional strip-loaded case for two reasons. In the first place, the complexity associated with a three-dimensional analysis would be excessive; the second reason is that anchorages in box section bridge girders would usually be located in the webs, which are thin, and therefore might be expected to show approximately planar behaviour. Thus, although the majority of experiments carried out in this field have been aimed at the three-dimensional case,[9–16] the resulting design recommendations are essentially two-dimensional in application. A detailed literature review on this subject is reported in ref. 17.

It was therefore decided to perform experiments on two-dimensional strip-loaded concrete prisms and to compare these results with the proposed two-dimensional methods of analysis. The behaviour of the test specimens could then be used to formulate and validate alternative analysis procedures. This Paper is thus the first in a series of three, and it provides the experimental results for reference by the subsequent papers, which look at plasticity analyses

of these results[18] and methods of designing general end-blocks using the plasticity principles applied in association with finite-element analysis.[19]

Test specimen details

In all tests the specimens had overall rectangular dimensions (h, $2a$, w) 750 mm × 250 mm × 125 mm. Such proportions and specimen size were chosen to be large enough to model the real problem, while allowing ease of laboratory handling and loading.

In all, seven series of tests were carried out. The specifications of the test specimens are outlined in Figs 1 and 2.

The series I specimens were unreinforced, mass concrete prisms.

The series II specimens contained rectangular steel stirrup reinforcement over a depth of $2a$ (250 mm). This reinforcement varied from 0·56 to 2·01% of the reinforced region. During series II testing it was found that fairly highly reinforced specimens (greater than 0·5% steel) underwent lateral expansion in the third direction under load. This caused out-of-plane failure so that a negligible increase in strength was obtained by increasing planar reinforcement percentages.

The series III specimens contained rectangular steel stirrup reinforcement identical to that used in series II. However, additional cross-links, tying the two stirrup-legs together, were used in this series; this maintained planar conditions, so that the study of the effect of reinforcement percentage on the prisms could continue.

The series IV specimens contained steel reinforcement located centrally within the prisms. These specimens were thus not aided in any way by the confinement contribution of rectangular stirrups (as was the case in series II and III).

The series V specimens were designed to investigate the influence of a duct hole on the strength of a prestressed concrete primary prism. The duct diameter was 25 mm in all these tests.

The series VI specimens contained steel stirrup reinforcement cages of varying length and steel percentage. Collins and Mitchell[20] suggested that beneficial behaviour might be obtained by spreading the steel stirrups over greater depths. Most of the steel was placed over the elastically highly stressed region (a depth of 1·6a),[20] and the rest of the steel over what remained of the reinforcement depth (3a or 4a), as shown in Fig. 3.

The series VII specimens (all unreinforced) contained an initial central 'crack', running axially from 50 mm below the loading plate to 50 mm above the basal platen. To achieve this, a 650 mm long, 0·8 mm thick, steel sheet was placed centrally in the formwork during casting. The sheet was removed after 24 hours, leaving an artificial crack in the prism. These specimens were tested to determine whether any energy was being dissipated in the central crack during collapse of the prisms, for use in the formulation of an upper-bound solution to the problem, as reported in a subsequent paper.[18]

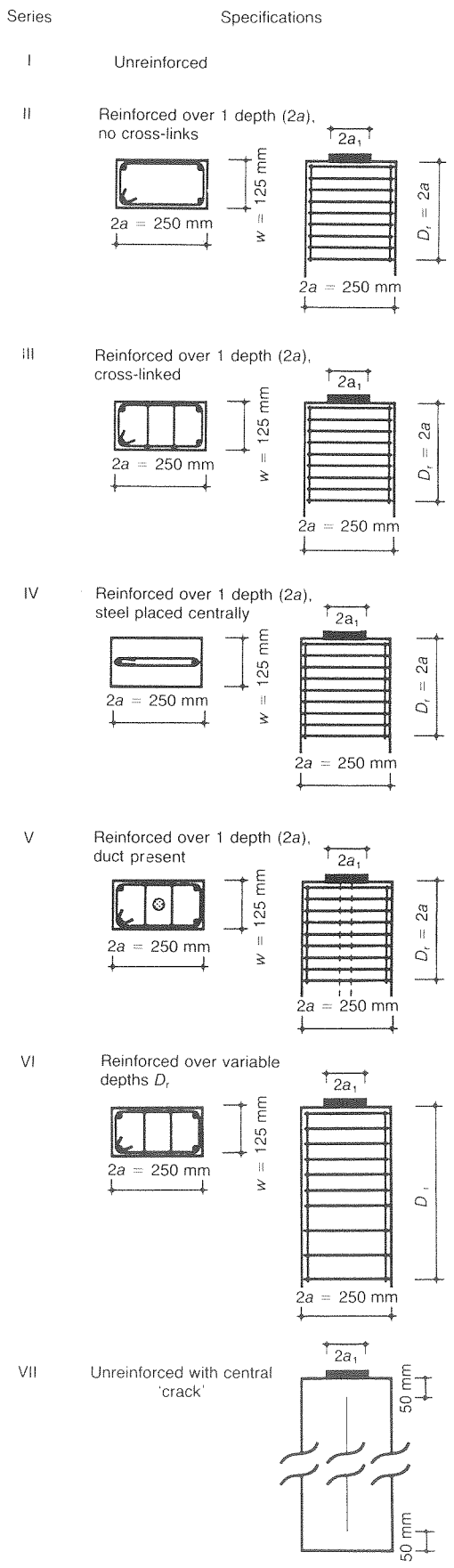

Fig. 1. Specification details for test specimens

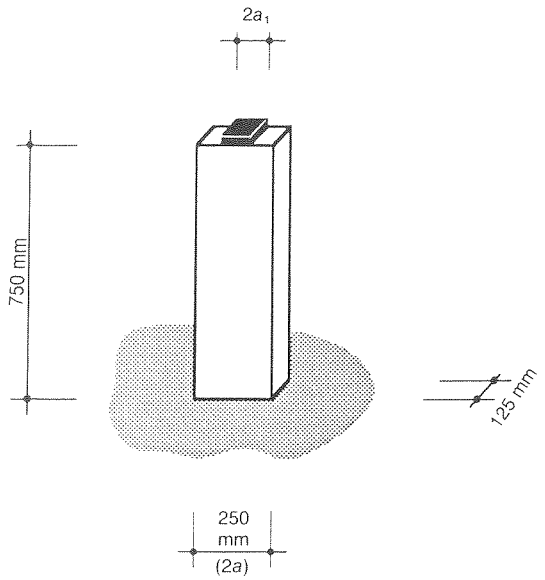

Fig. 2. Overall dimensions of test specimens

All specimens were strip-loaded through rigid 25 mm thick steel plates of width 125 mm. Such a loading was assumed to represent satisfactorily the transfer of force from cable to concrete at an anchorage in a prestressed concrete structure. The loading plates were placed centrally on the specimens, with a thin layer of gypsum plaster separating steel from concrete, allowing an even distribution of load. The ratio of loaded length $2a_1$ to total length $2a$ was varied between 0·1 and 0·7 to produce a spread of results applicable to primary prism loadings.

To determine the effects of steel reinforcement on the behaviour of the prisms, rectangular steel stirrups were cast into several specimens (see Fig. 1). The stirrups were bent from either 2·4, 4·0 or 6·1 mm diameter mild steel bars. From load–strain plots, taking the 0·2% proof strain as the yield strength of each bar, the following values were obtained

(*a*) 2·4 mm diameter, f_y = 429 N/mm^2
(*b*) 4·0 mm diameter, f_y = 417 N/mm^2
(*c*) 6·1 mm diameter, f_y = 438 N/mm^2.

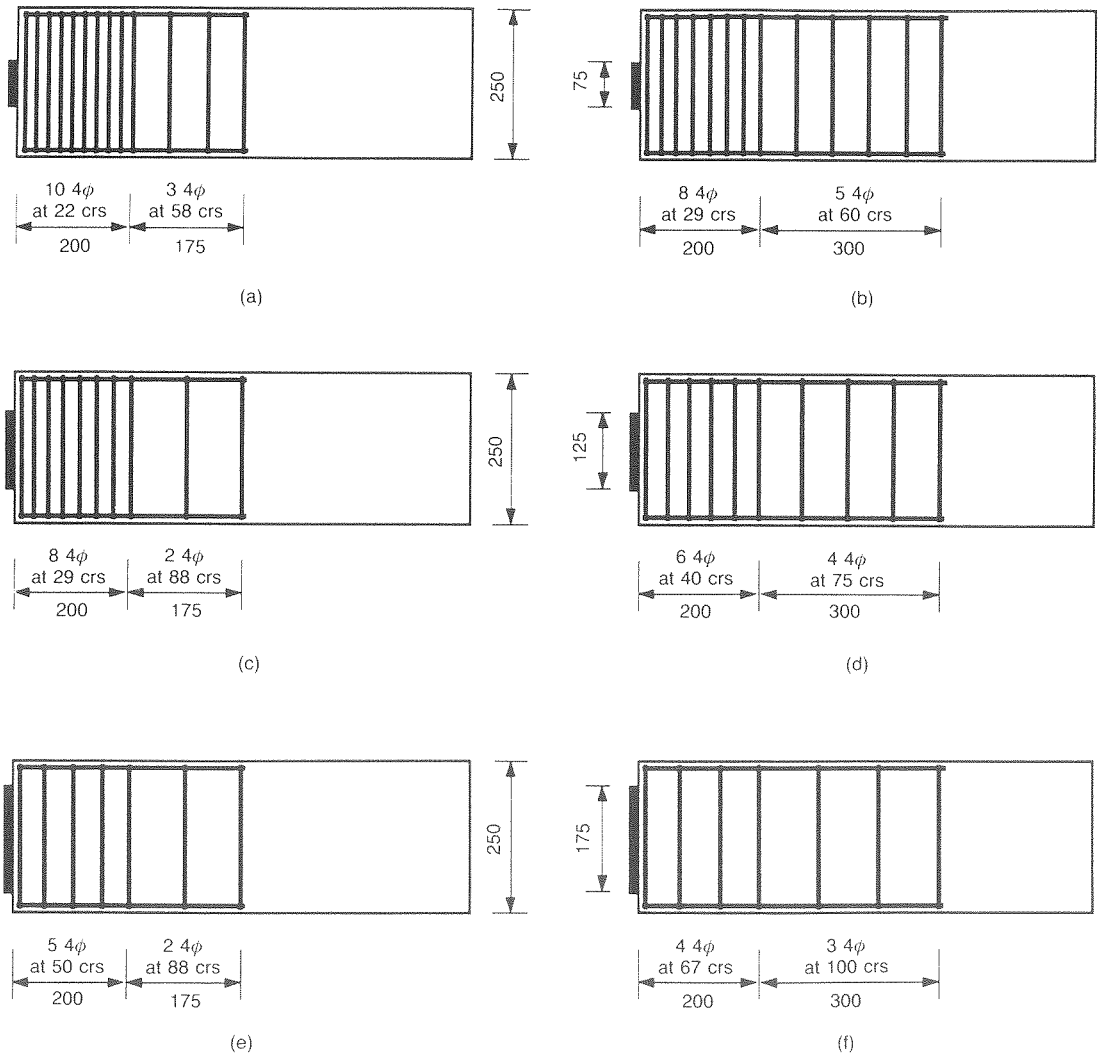

Fig. 3. Configurations of steel reinforcement for series VI specimens: (a) 10033aS-4; (b) 10034aS-4; (c) 08053aS-4; (d) 08054aS-4; (e) 050073aS-4; (f) 05074aS-4 (dimensions in mm)

The stirrups were spot-welded to closure in every case to prevent the possibility of bond-slip, and they were assembled on to four 4·0 mm diameter longitudinal bars to form cages. These cages were of varying length, as shown in Fig. 1. The minimum cover all round the stirrup steel was always 10 mm, regardless of the bar size. The commonly accepted bursting region in primary prisms is of dimensions $2a$ in depth and w in width. Therefore, the steel reinforcement quantity is in every case expressed as a percentage of the area $2aw$, even when the steel stirrups were placed over depths other than $2a$. Such percentages of steel ranged from 0% to about 2% in the tests.

It will be convenient to define another measure of the amount of steel present, which takes account of the depth over which the steel is distributed. The steel parameter Φ is defined as

$$\Phi = \frac{A_s f_y}{D_r w f_{cu}} \qquad (1)$$

where A_s is the total area of reinforcement across the central crack plane (both stirrup legs included), f_y is the yield strength of the steel bars, D_r is the depth of reinforcement, w is the width of the specimen (125 mm in all cases), and f_{cu} is the compressive cube strength of the concrete.

In several reinforced specimens, electrical resistance strain gauges were fixed to the steel reinforcing stirrups. The strain gauges were 3 mm long and of type TML-FLA-3-11. They were placed centrally along one leg of each stirrup, so that the variation in strain along the axis of the loaded specimen might be recorded.

The specimens were cast in a horizontal position in a timber mould that produced three specimens at each pour.

The strength of the concrete in most prestressed concrete structures is usually higher than that in reinforced concrete structures. Consequently, it was decided to use a fairly high strength concrete (about 60 N/mm^2 cube compressive strength). Moreover, owing to time constraints, it was necessary for this strength to be achieved at age seven days, so that many specimens could be tested over a short period. The mix proportions chosen for the concrete were: stone 1030 kg/m^3 (10 mm rounded river gravel); sand 683 kg/m^3 (5 mm (max.) natural glacial); cement 545 kg/m^3 (ordinary Portland); water 186 kg/m^3; plasticizer 5·31 l/m^3 (Supaflo).

A stress–strain curve for the concrete was found by testing a 200 mm × 100 mm concrete cylinder in a displacement-control Avery-Denison compression testing machine. The initial Young's modulus for the concrete was found to be about 28 kN/mm^2 at seven days.

The control specimens for each batch of three prisms consisted of two 100 mm cubes, and one 200 mm × 100 mm cylinder, for determination of the compressive and split-tensile strengths of the concrete, respectively. Both the test and control specimens were demoulded after 24 h and left for four days to cure under damp hessian cloth and plastic sheeting. The test specimens were then painted, connected to data loggers and tested on the seventh day.

A 250 t load range on a load-controlled Amsler compression testing machine was used for all tests. A thin layer of gypsum plaster was placed between the base of the specimen and the lower platen of the machine, to ensure a uniform distribution of load. Care was taken to ensure both vertical and horizontal alignment of the specimens in the machine.

Strain readings (from those specimens containing strain gauges) were collected on an Orion data-logger at 5 t intervals during loading.

The load to cause first cracking was noted, as was the ultimate load for each specimen. Crack propagation directions and rates were also noted. Initial cracking was detected purely by visual inspection of the specimens at intermittent load levels.

All specimens have associated codes to distinguish them. These codes have the following format for series I–III

ppcc-d

where *pp* is the percentage steel present over depth $2a$ (e.g. 05 is 0·5%), *cc* is the concentration ratio a_1/a (e.g. 03 is $a_1/a = 0{\cdot}3$), and *d* is the diameter of the steel bar used, to the nearest millimetre.

In series IV and V, the *C* and *D* symbols represent 'central steel positioning' and 'ducted prism', respectively, as described in Fig. 1. The formats for these two series are thus

ppccC-d or *ppccD-d*

where *pp*, *cc* and *d* are as defined above.

In series VI, the format is

ppccNaE-d or *ppccNaS-d*

where *Na* is the depth to which the steel is placed ($2a$ = 250 mm), *E* means that the stirrups are evenly spaced, *S* means that the stirrups are spread out non-uniformly, and *pp*, *cc* and *d* are as defined above.

The format for series VII is

ppccI

where *I* means that the prism has a initial central 'crack' along its axis.

Experimental results

Table 1 shows a detailed summary of all the tests carried out in the seven series of experiments.

To be able to compare the enhancement in strength of the prisms due to steel reinforcement with enhancement in strength due to surrounding concrete, a notional value P_0 of load is introduced. P_0 is defined as that load which would cause compression failure of a full-face loaded unreinforced concrete column of dimensions $2a_1$ × 125 mm × 750 mm. Such a test on a specimen of dimensions 250 mm × 125 mm × 750 mm produced an

Table 1. Summary of all results from testing programme

Series	Specimen code	Concentration ratio a_1/a	No. of stirrups	Diameter of stirrups: mm	Depth of reinforcing D_r: mm	f_{cu}: N/mm^2	f_t': N/mm^2	$\phi=\frac{A_s f_y}{D_r w f_{cu}}$	Cracking load P_{cr}: t	Ultimate load P: t	$k_c=P/P_0$
I	0001	0·1	—	—	—	60·3	3·88	0	30	30	2·38
	0003	0·3	—	—	—	63·1	4·12	0	45	50	1·26
	0005	0·5	—	—	—	62·3	3·53	0	66	72	1·10
	0007	0·7	—	—	—	63·1	4·39	0	90	96	1·04
	0010	1·0	—	—	—	62·7	3·95	0	132	132	1·00
II	0503-4	0·3	7	4	250	55·7	4·07	0·0422	59	69	1·97
	1003-4	0·3	13	4	250	61·1	4·32	0·0714	70	76	1·98
	1503-6	0·3	8	6·1	250	56·2	3·72	0·117	70	78	2·21
	0505-4	0·5	7	4	250	59·6	4·27	0·0394	87	92	1·47
	1005-4	0·5	13	4	250	64·9	4·24	0·0672	101	111	1·63
	1505-6	0·5	8	6·1	250	56·6	3·70	0·116	102	108	1·82
	0507-4	0·7	7	4	250	62·1	4·35	0·0378	125	125	1·37
	1007-4	0·7	13	4	250	61·5	3·90	0·0709	128	133	1·48
	1507-6	0·7	8	6·1	250	62·1	4·55	0·105	135*	135*	1·48*
III	0501-4	0·1	7	4	250	60·3	3·88	0·0389	30	37	2·93
	1001-4	0·1	13	4	250	60·3	3·88	0·0723	32	42	3·33
	0503-4	0·3	7	4	250	60·0	4·22	0·0392	60	70·5	1·87
	1003-4	0·3	13	4	250	60·2	4·02	0·0724	77	88·5	2·34
	0503-6	0·3	3	6·1	250	59·5	4·02	0·0413	65	74·5	1·99
	1003-6	0·3	6	6·1	250	55·2	3·77	0·089	74	82	2·37
	1503-6	0·3	8	6·1	250	59·6	4·11	0·11	80	90	2·41
	2003-6	0·3	11	6·1	250	61·1	4·01	0·148	82	101	2·63
	0503-2	0·3	20	2·4	250	60·0	3·96	0·0414	65	71	1·88
	0505-4	0·5	7	4	250	60·0	4·22	0·0392	81	91·5	1·46
	0805-4	0·5	10	4	250	59·5	4·02	0·0564	96	103	1·65
	1005-4	0·5	13	4	250	60·2	4·02	0·0724	105	115	1·83
	1505-6	0·5	8	6·1	250	61·1	4·01	0·1080	119	128	2·00
	0505-6	0·5	3	6·1	250	59·5	4·02	0·0413	90·5	100	1·61
	1005-6	0·5	6	6·1	250	55·2	3·77	0·089	101	107	1·85
	0405-2	0·5	15	2·4	250	60·0	3·96	0·0311	79	87	1·39
	0307-4	0·7	3	4	250	59·5	4·02	0·0169	98	104	1·19
	0507-4	0·7	7	4	250	60·0	4·22	0·0392	121	124·5	1·42
	0807-4	0·7	10	4	250	61·1	4·01	0·0549	127	132	1·47
	0507-6	0·7	3	6·1	250	59·5	4·02	0·0413	118	127·5	1·46
	1007-6	0·7	6	6·1	250	55·2	3·77	0·089	131	131	1·62
	0307-2	0·7	10	2·4	250	60·0	3·96	0·0207	105	108	1·23
IV	0503C-4	0·3	7	4	250	58·3	4·14	0·0403	56·5	60·5	1·65
	0505C-4	0·5	7	4	250	58·3	4·14	0·0403	75	84·5	1·38
	0507C-4	0·7	7	4	250	58·3	4·14	0·0403	104	110·5	1·29
V	0003D	0·3	—	—	—	59·4	4·31	0	39·5	49	1·31
	0005D	0·5	—	—	—	59·4	4·31	0	59	70	1·13
	0007D	0·7	—	—	—	59·4	4·31	0	85·5	91·5	1·05
	1003D-4	0·3	13	4	250	61·4	4·07	0·071	72	85	2·20
	0805D-4	0·5	10	4	250	69·0	3·96	0·0486	91·5	100·5	1·39
	0507D-4	0·7	7	4	250	69·0	3·96	0·034	114	118·5	1·17
VI	100316aE-4	0·3	13	4	200	58·5	4·22	0·0932	70·5	73	1·99
	080516aE-4	0·5	10	4	200	58·5	4·22	0·0717	83	90	1·47
	050716aE-4	0·7	7	4	200	58·5	4·22	0·0502	99·5	108	1·26
	10033aE-4	0·3	13	4	375	60·8	4·28	0·0478	78	84	2·20
	08053aE-4	0·5	10	4	375	60·8	4·28	0·0368	93·5	105·5	1·66
	05073aE-4	0·7	7	4	375	60·8	4·28	0·0257	130	132	1·48
	10033aS-4	0·3	13	4	375	60·6	4·41	0·048	75	83	2·18
	08053aS-4	0·5	10	4	375	60·6	4·41	0·0369	95·5	101	1·59
	05073aS-4	0·7	7	4	375	60·6	4·41	0·0258	112·5	117	1·32
	10034aE-4	0·3	13	4	500	59·9	3·97	0·0364	55	69·5	1·85
	08054aE-4	0·5	10	4	500	59·9	3·97	0·028	75	94	1·50
	05074aE-4	0·7	7	4	500	59·9	3·97	0·0196	94·5	114	1·30
	10034aS-4	0·3	13	4	500	55·9	3·96	0·039	57·5	71	2·02
	08054aS-4	0·5	10	4	500	55·9	3·96	0·03	74·5	92	1·57
	05074aS-4	0·7	7	4	500	55·9	3·96	0·021	92	107	1·31
VII	0001I	0·1	—	—	—	61	4·11	0	—	22	1·72
	0003I	0·3	—	—	—	61	4·11	0	—	56	1·46
	0005I	0·5	—	—	—	61	4·11	0	—	70	1·10

* Lower concrete failed in compression

ultimate load of 132 t when the cube strength of the concrete was $62{\cdot}7\ \mathrm{N/mm^2}$. The compressive failure stress of the specimen was thus about $0{\cdot}67f_{cu}$. Hence, the notional load is defined as $P_0 = 2a_1 \times 125\,\mathrm{mm} \times (0{\cdot}67f_{cu})$, for each particular specimen. The ratio of the ultimate load P obtained from the tests to the notional load P_0 then represents the total enhancement in strength k_c that is derived from the surrounding concrete and steel reinforcement.

Series I

The series I specimens were tested to assess the unreinforced bursting resistance of mass concrete prisms. In addition, it was important to study the modes of failure of these specimens, so that suitable reinforcement schemes could be developed for the subsequent test series.

The concentration ratio a_1/a was varied between $0{\cdot}1$ and $1{\cdot}0$, so that a large spread of possible loading cases was covered.

For $a_1/a = 1{\cdot}0$, failure of the prism occurred suddenly, with no prior cracking. An inclined slip-plane was formed diagonally across the specimen at failure. This failure occurred in-plane.

For all other concentration ratios, however, initial cracking preceded ultimate failure. At first, a vertical crack formed at the point of maximum lateral tensile stress on the central axis of the specimens. This point varied between concentration ratios, but was usually about $100-150\,\mathrm{mm}$ $(0{\cdot}8a-1{\cdot}2a)$ below the loading plate.

For $a_1/a = 0{\cdot}1$, propagation of this crack occurred almost instantaneously at constant load. The crack extended towards both the loading plate and the base. A redistribution of stress in the region immediately below the loading plate must have occurred to maintain equilibrium. Such conditions of stress led to immediate wedging failure punch-through, as shown in Fig. 4(a).

For a_1/a greater than $0{\cdot}1$, failure occurred in an obvious two-step process. Initial central cracking occurred as before. Propagation of this crack occurred in both directions in a controlled manner, under steadily increasing load. The central crack terminated about 25 to 50 mm below the loading plate, and between 50 and 200 mm above the base. At a higher load, wedging punch-through of the plate occurred (see Fig. 4(b)). In all unreinforced cases, the wedging failure itself was sudden, with no inclined cracks forming prior to ultimate collapse.

Series II

The probable mode of failure for series II tests had been established from the previous series. However, it was found that the quantity of primary steel reinforcement present in the specimens affected the ultimate failure mode of the prisms. It is useful, therefore, to distinguish between the behaviour of lightly reinforced prisms and that of more heavily reinforced ones.

Lightly reinforced specimens. Up to a steel parameter of about $\Phi = 0{\cdot}04$ (steel percentage of about $0{\cdot}5\%$), failure of all the specimens occurred in a two-step process,

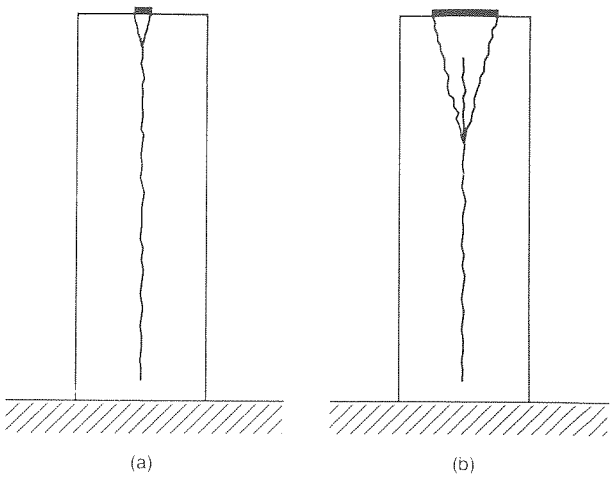

Fig. 4. Planar wedge failures of series I specimens: (a) $a_1/a = 0{\cdot}1$; (b) $a_1/a > 0{\cdot}1$

as for the unreinforced cases. A small initial vertical crack occurred along the central axis of the prism at the position of maximum lateral tensile stress. The load at which the crack became visible was considerably higher than the corresponding load in the unreinforced case for every a_1/a ratio (see column 10 of Table 1). Gradual propagation of this crack occurred along the length of the specimen, as for the unreinforced case. Incompatibility cracks started to occur, both parallel to, and immediately below the edges of the loading plate, at the same time. Failure occurred soon after this. The actual failure was brittle in nature, with a wedge punch-through occurring as for the unreinforced cases.

As wedging failure occurred, it was noticed in all cases that the two outer blocks (B and C in Fig. 5) rotated outwards about the base to allow the wedge to penetrate

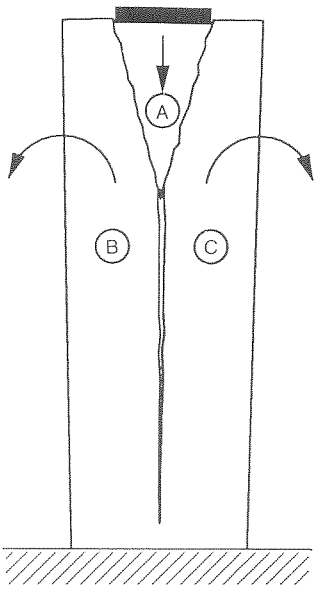

Fig. 5. Wedge action causing tapering of central crack and rotation of two outer blocks

the prism. This means that the basal conditions might have played a part in the behaviour of the prisms, as the central crack in no case extended right down to the base platen.

From Table 1 it is quite clear that light reinforcement increased the strength of the prisms substantially. Enhancement factors show a sharp increase for all concentration ratios for values of Φ up to about 0·04.

Heavily reinforced specimens ($\Phi > 0{\cdot}04$ approximately). Initial cracking occurred as before along the central axis of the prism, ostensibly at the position of maximum bursting tensile stress. As the load increased, however, propagation of this crack was extremely slow and only directed towards the base. Maximum lengths of such cracks at failure were about 100–200 mm.

Collapse consisted of wedging in the lateral (third) direction, as shown in Fig. 6. This out-of-plane failure was caused by insufficient reinforcement in the third direction to bind the concrete together beneath the plate. The initial cracking which had been seen on the surface of the prism had probably not been of bursting origin, but rather was due to out-of-plane expansion incompatibility. The fact that it occurred at the position of maximum planar bursting stress may be coincidental.

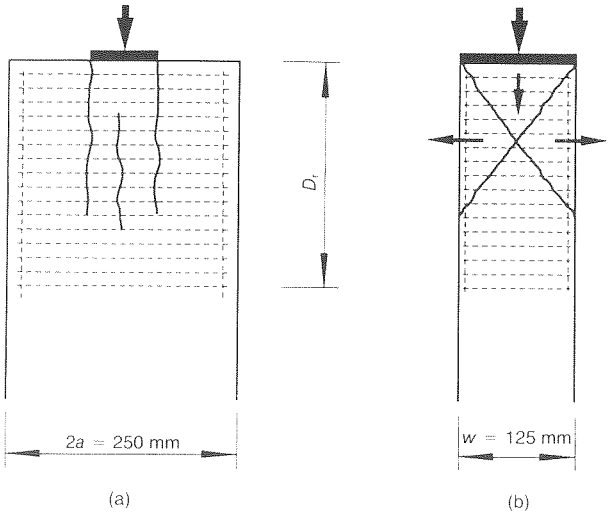

Fig. 6. Out-of-plane wedging failure in highly reinforced prisms: (a) front view; (b) side view

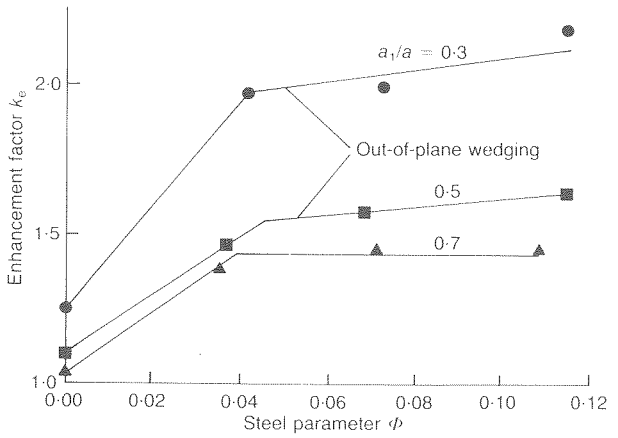

Fig. 7. Plot of enhancement factor k_e against steel parameter Φ for series II

As the level of primary stirrup reinforcement was increased, insignificant additional strength was obtained from these prisms, as can be seen from Table 1 and from Fig. 7, which shows the enhancement fact k_e plotted against the steel parameter Φ for all levels of reinforcement for series II tests (results from series I for $\Phi = 0$ are also included).

It became obvious that confinement of the concrete below the wedging plate was essential to increase the bearing capacity and to allow development of the full planar bursting strength of the prisms.

Series III

The series III specimens were designed to overcome the out-of-plane wedging failures encountered in series II and to allow the continuation of planar behaviour for increasing steel percentages. For the 4·0 mm diameter bar stirrups, two cross-links, also of 4·0 mm steel, were added to each rectangular stirrup to tie the parallel legs together and reduce the possibility of out-of-plane expansion and wedging. For the 6·1 mm diameter bar stirrups, two pairs of 4·0 mm diameter bar cross-links were used, to avoid sharp bends in the larger bars.

This reinforcement arrangement turned out to be successful in part, with no out-of-plane wedging occurring in lightly-to moderately reinforced prisms ($\Phi \leq 0{\cdot}07$ approximately) for $a_1/a > 0{\cdot}1$. However, lateral out-of-plane expansion was not entirely prevented for high reinforcement percentages. Failure in these cases was again by out-of-plane wedging, caused by the reduction in third-direction confinement as the cross-links yielded. Fig. 8 shows a plot of the enhancement factor k_e against the steel parameter Φ for all levels of reinforcement for the series III tests.

Below Φ of 0·07 the strengths of the specimens increased linearly, but the rate of strength increase reduced significantly above $\Phi = 0{\cdot}07$.

Figure 9 shows a photograph of typical planar wedge failures of two series III specimens, 0507-4 and 0507-6. The wedge formation and central crack may be seen in these specimens.

It was found that for specimens with a_1/a greater than 0·1, the maximum strain in the most highly stressed steel stirrup at visible cracking loads was between 1200 and 1800 $\mu\epsilon$, corresponding to a maximum stress between 240 and 360 N/mm^2. For $a_1/a = 0{\cdot}1$, the maximum strain was about 600 $\mu\epsilon$ at cracking. These strains are much higher than might be expected from a simple tensile strain cut-off failure criterion for concrete, a finding similar to that of Taylor.[15] It appears that although microcracking would have started earlier than reported, the presence of the steel helped substantially to delay the visible cracking of the specimens. The intermittent monitoring of the specimens for cracking would, however, have led to overestimates of the visible cracking capacities of the prisms.

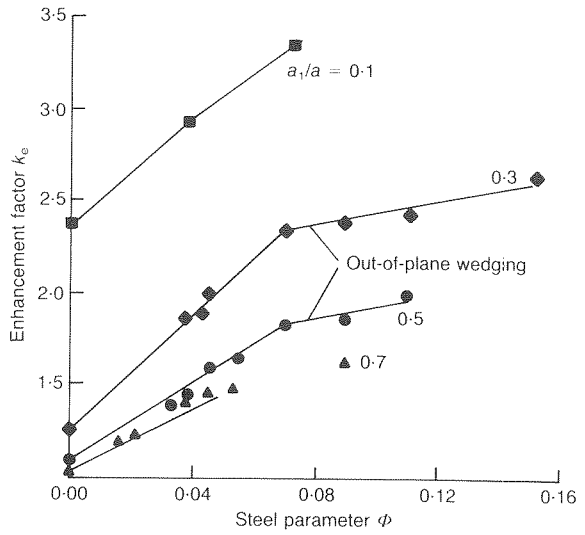

Fig. 8. Plot of enhancement factor k_e against steel parameter Φ for series III

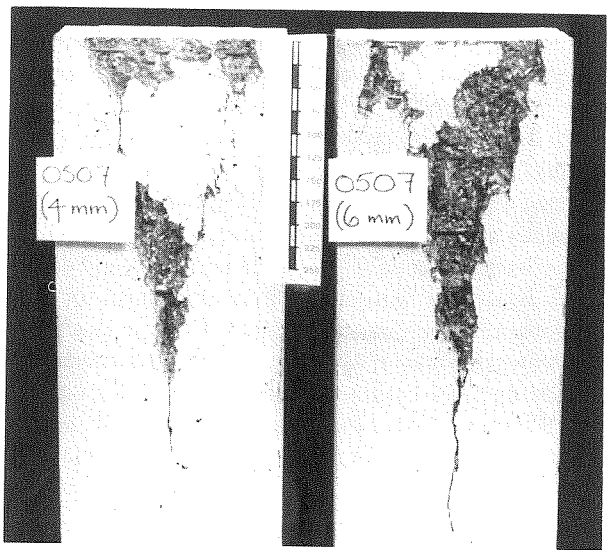

Fig. 9. Failure zones of specimens 0507-4 and 0507-6 showing typical crack patterns and wedge formation

Non-linear behaviour of the specimens (based on measured steel strains) was found to be initiated when the strain in the most highly stressed steel bar was about 260 $\mu\epsilon$, which is close to the accepted cracking strain capacity of concrete.[17] It may thus be concluded that microcracking and non-linear behaviour of the prisms occurred when the concrete reached its maximum tensile strain limit, but that visible cracking occurred at higher strains.

Series IV

In order to gauge the effect of confinement due to the rectangular stirrups of series II, steel reinforcement was placed centrally. All failures in this series were caused by out-of-plane third-direction wedging beneath the loading plate, as found in heavily reinforced series II specimens.

Both the cracking and ultimate loads were significantly lower than those found in specimens of series II and III with similar steel percentages, where some confinement was created by the rectangular stirrups (see Table 1). It is reasonable to conclude that the rectangular stirrups employed in the other test series helped to create plane strain conditions across the prism.

Series V

A 25 mm diameter duct hole was located centrally down the length of series V specimens, which represented a 1·6% loss in material over the entire cross-section.

The loss in strength of the reinforced ducted specimens over the corresponding solid prism specimens was greater than the loss in cross-sectional area due to the duct hole. This is significant, as it is assumed at present that the duct hole may simply be treated as a loss in cross-sectional area of a primary prism for design purposes.[16]

Much resistance to cracking is lost with the presence of a duct. It seems likely, therefore, that it is unreasonable simply to assume a loss in cross-sectional area to account for the presence of a duct hole. There are three-dimensional effects occurring within the specimens which must complicate the problem of predicting the strength of such ducted prisms. However, the mode of failure was the same as before, with a stable central crack forming, followed by wedging failure.

Series VI

Collins and Mitchell[20] proposed that it would be beneficial in primary prism design to spread steel out, perhaps non-uniformly, over a depth greater than the conventional $2a$.

Steel was spread over 200 mm (1·6a), 375 mm (3a) and 500 mm (4a), both uniformly (even spacing of stirrups) and non-uniformly (more steel placed in the elastically highly stressed region, the rest placed over what remained of D_r). It was decided to place about 1% steel in specimens with a_1/a = 0·3, 0·8% steel in specimens with a_1/a = 0·5, and 0·5% steel in specimens with a_1/a = 0·7. These quantities of steel would certainly allow planar wedging failure to occur in each specimen and permit several stirrups to be used, so that the non-uniform spreading of reinforcement over varying depths could be adequately studied.

All failures in this series consisted of initial central cracking, followed by planar wedging failure at a higher load. Rotation of the surrounding outer blocks caused tapering of the central crack to occur at failure.

Figure 10 shows the variation in the enhancement factor k_e, obtained for a_1/a ratios of 0·3, 0·5 and 0·7, plotted against the depth over which the steel was placed. With the exception of specimens with a_1/a = 0·3, there seems to be little difference in strength between prisms reinforced over depth $2a$ and those reinforced over depth $3a$. Fig. 11 shows the variation in visible cracking load capacity of the prisms with the depth of reinforcement for various a_1/a ratios.

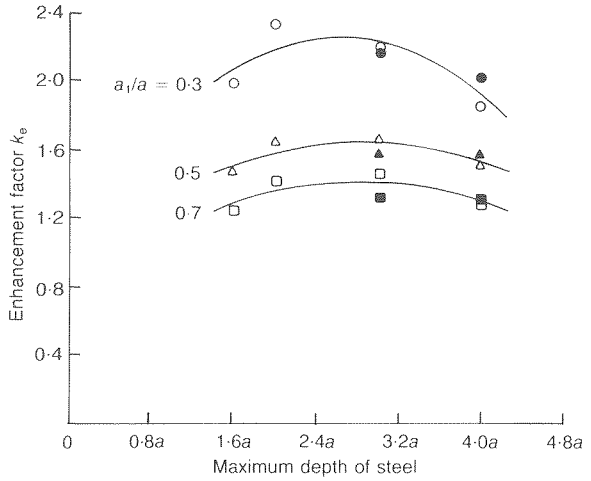

Fig. 10. Variation of enhancement factor k_e against depth of reinforcing into prism for several a_1/a ratios. Quantity of steel is constant for each a_1/a ratio. Open symbols represent specimens with evenly spaced stirrups, solid symbols represent uneven spacing.

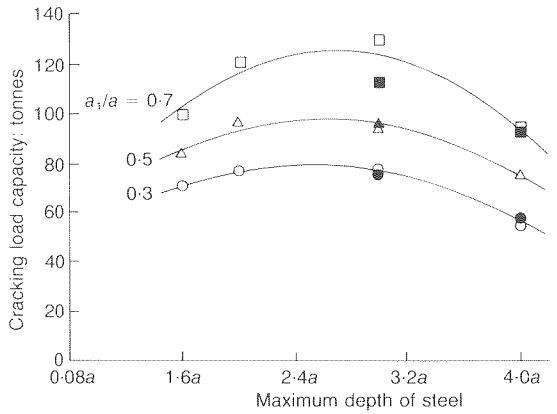

Fig. 11. Variation of cracking loads obtained from testing, with depth of reinforcing, for several a_1/a ratios

The general shape of the plots in Figs 10 and 11 may be explained as follows. When steel was placed over depth $1{\cdot}6a$ only, initial cracking was observed at the base of the reinforcing cage. This is because the tensile stress existing at this location exceeded the unreinforced tensile capacity of the concrete, as predicted by Collins and Mitchell. This premature cracking propagated along the prism. The unrestricted opening of this crack below the base of the reinforcement caused such a loss in stiffness, and a resultant redistribution of stress below the loading plate, that wedging failure occurred earlier than might have been expected. When steel was placed over depth $4a$, the reduction in steel concentration over the bursting region resulted in low cracking load and ultimate capacities, as expected.

It is not clear why the cracking loads for specimens reinforced over depths $2a$ and $3a$ should have been of similar magnitude, as initial cracking in both these cases occurred within the reinforced region. For specimens with steel spread over $3a$ depth, however, the opening of this crack would have been restricted for a greater depth than in the specimen reinforced over depth $2a$. This would have helped to prevent loss in stiffness of the prism and possibly aided its ultimate load capacity. With steel spread over depth $3a$, however, the wedging planes would have crossed fewer steel bars, negating this strength enhancement.

It does seem possible, therefore, that there exists an optimum depth of reinforcement, somewhere between $2a$ and $3a$ in length, at which maximum advantage may be obtained from the given quantity of steel. It appears that there is little strength penalty paid for spreading the steel over depth $3a$, instead of over $2a$. However, many more tests would be necessary to confirm the above postulates fully.

Series VII

Three tests were carried out in this series to determine whether significant energy was dissipated along the central crack during ultimate collapse. To achieve this, unreinforced, artificially cracked specimens were tested to ultimate collapse.

With the exception of $a_1/a = 0{\cdot}1$, similar ultimate strengths were obtained in the two series. It is therefore unlikely that any significant energy was dissipated along the central crack during the collapse of series I specimens. The fact that specimen 0003I failed at a load above that of specimen 0003 is inexplicable, and is attributed to exceptional scatter.

For $a_1/a = 0{\cdot}1$, it was noticed during series I testing that ultimate wedging failure occurred at the same time as the appearance of the initial crack. It is therefore likely that the strength of this specimen was derived principally from the splitting resistance of the prism. With the presence of the crack from the start of the test, this resistance was removed, and the strength of the prism was governed by the wedging resistance of the split prism.

Comparison of results with literature

Several areas of interest exist for comparison between the experimental results and existing theories and design methods.

Bursting strain readings from the tests carried out were found to be in close agreement with linear elastic finite-element (FE) predictions at low loads. Corresponding bursting stress distributions from the FE analyses were then compared with existing theories[3,6,16,21,22] and good agreement was again obtained. The only exception to this was with the results of Zielinski and Rowe[16] which predicted significantly higher stresses than those found during this research.

Figure 12 shows plots of the predicted design load capacities by several methods[5,8,16,21,22] against the steel parameter Φ for the present test specimens, with $a_1/a = 0{\cdot}3$. The load capacity from each method is considered to be either the cracking or the ultimate load, whichever is less, for the given amount of steel present. The

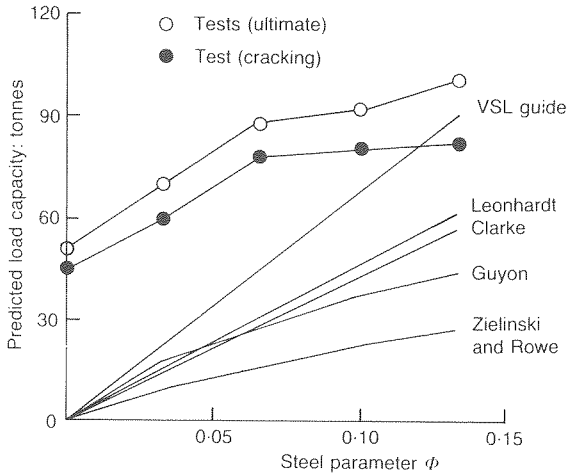

Fig. 12. Predicted design load capacities of test specimens for $a_l/a = 0{\cdot}3$

experimental results from series III are plotted for comparison. An allowable concrete tensile strength of $2{\cdot}48\ N/mm^2$ has been assumed for use in Guyon's and Zielinski and Rowe's methods, in accordance with ref. 23, assuming $f_{cu} = 60\ N/mm^2$.

Two interesting points are evident from these plots.

In comparison with the other methods and test results, the method due to Zielinski and Rowe (which is in general use in the UK for bursting zone design) is somewhat conservative for the estimation of required reinforcement in the bursting zone of such planar specimens. The placement of an excessive quantity of steel in a primary prism causes severe congestion problems, leading to poor-quality compaction of concrete in this highly stressed region.

None of the design methods allows any significant portion of the tension to be carried by the concrete when designing the reinforcement. The design methods of Zielinski & Rowe and Guyon both include an allowable tensile strength of concrete, but they negate this by allowing very low stresses in the steel. It appears from Fig. 12 that more use could be made of the inherent strength of the concrete, particularly for low steel parameters, judging by the separation of the design curves from the experimental results in this region.

Conclusions

Many experiments have been undertaken in attempts to study the behaviour of strip-loaded reinforced concrete prisms. The general failure modes of the prisms have been studied and compared with existing literature on the subject. The following main conclusions are drawn from this study.

Reasonable agreement with other methods has been achieved in terms of stress and strain variation at low loads. However, it has been shown that the present methods used in the design of the reinforcement for primary prisms are generally very conservative. Although it is appreciated that design methods must, through necessity, be conservative, the over-reinforcing of a primary prism is problematic, as congestion may occur in this critical and highly stressed region.

A possible solution to this congestion would be to spread the steel reinforcement out over a greater depth than that presently used. It was found that there could be some benefit gained in terms of cracking and ultimate load capacities through such action.

The occurrence of out-of-plane behaviour in such strip-loaded specimens may be of significance in practice, particularly where insufficient spiral reinforcement is placed around an anchorage which is designed according to a planar failure mechanism.

Acknowledgements

The experimental work was carried out in the Cambridge University Engineering Department. The technical assistance of Mr C. J. Mason and Mr V. L. Piper is gratefully acknowledged.

References

1. Guyon Y. *Prestressed concrete*. F. J. Parsons, London, 1953.
2. Hawkins N. M. The bearing strength of concrete for strip loadings. *Mag. Concr. Res.*, 1970, **22**, 87–98.
3. Iyengar K. T. S. R. Two-dimensional theories of anchorage zone stresses in post-tensioned prestressed beams. *J. Am. Concr. Inst.*, 1962, **59**, 1443–1465.
4. Lenschow R. J. and Sozen M. A. Practical analysis of the anchorage zone problem in prestressed beams. *J. Am. Concr. Inst.*, 1965, **62**, 1421–1438.
5. Leonhardt F. *Prestressed concrete — design and construction*. Wilhelm Ernst, Berlin, 1964.
6. Magnel G. Design of the ends of prestressed concrete beams. *Conr. Constr. Engng*, 1949, **44**, 141–148.
7. VSL International. *End block design in post-tensioned concrete*. Berne, 1975.
8. VSL International. *Detailing for post-tensioning*. VSL report series 3. Berne, 1991.
9. Au T. and Baird D. L. Bearing capacity of concrete blocks. *J. Am. Concr. Inst.*, 1960, **31**, 869–879.
10. Ban S. *et al.* Anchorage zone stress distributions in post-tensioned concrete members. *Proc. world conf. prestressed concrete*. San Francisco, 1957, 16-1–16-14.
11. Middendorf K. H. Practical aspects of end zone bearing of post-tensioning tendons. *J. Prestressed Concr. Inst.*, 1963, **8**, 57–62.
12. Niyogi S. K. Concrete bearing strength — support, mix, size effect. *J. Struct. Div. Am. Soc. Civ. Engrs*, 1974, **100**, 1685–1702.
13. Niyogi S. K. Bearing strength of reinforced concrete blocks. *J. Struct. Div. Am. Soc. Civ. Engrs*, 1975, **101**, 1125–1137.
14. Shelson W. Bearing capacity of concrete. *J. Am. Concr. Inst.*, 1957, **29**, 405–414.
15. Taylor S. J. Anchorage bearing stresses. *Conf. on prestressed concrete pressure vessels*. Institution of Civil Engineers, London, 1967, 563–576.
16. Zielinski J. and Rowe R. E. *An investigation of the stress distribution in the anchorage zones of post-tensioned concrete members*. Cement and Concrete Association Research Report 9, 1960.
17. Ibell T. J. *Behaviour of anchorage zones for prestressed concrete*. PhD dissertation, University of Cambridge, 1992.

18. IBELL T. J. and BURGOYNE C. J. A plasticity analysis of anchorage zones. *Mag. Concr. Res.*, 1994, to be published.
19. IBELL T. J. and BURGOYNE C. J. A generalized lower bound analysis of anchorage zones. *Mag. Concr. Res.*, 1994, to be published.
20. COLLINS M. P. and MITCHELL D. *Prestressed concrete basics*. Canadian Prestressed Concrete Institute, Ontario, 1987.
21. CLARKE J. L. *A guide to the design of anchor blocks for post-tensioned prestressed concrete*. CIRIA, London, 1976.
22. GUYON Y. *Limit-state design of prestressed concrete:* Volume 2: The design of the member. Applied Science Publishers, London, 1974.
23 DEPARTMENT OF TRANSPORT. *Prestressed concrete for highway structures*. Technical memorandum (bridges) BE 2/73 (3rd amendment). London, 1975.

Discussion contributions to this Paper should reach the Editor by 30 June 1994